Surface deformation during the Mw 6.4 (8 June 2008) Movri Mountain earthquake in the Peloponnese, and its implications for the seismotectonics of western Greece

Article *in* International Geology Review · February 2010

DOI: 10.1080/00206810802674329

CITATIONS
28

READS
94

3 authors:

Ioannis Koukouvelas
University of Patras
109 PUBLICATIONS **1,865** CITATIONS
SEE PROFILE

Sotirios Kokkalas
Khalifa University
70 PUBLICATIONS **1,003** CITATIONS
SEE PROFILE

P. Xypolias
University of Patras
69 PUBLICATIONS **1,102** CITATIONS
SEE PROFILE

International Geology Review
Publication details, including instructions for authors and subscription information:
http://www.informaworld.com/smpp/title~content=t902953900

Surface deformation during the Mw 6.4 (8 June 2008) Movri Mountain earthquake in the Peloponnese, and its implications for the seismotectonics of western Greece

Ioannis K. Koukouvelas [a]; Sotirios Kokkalas [a]; Paraskevas Xypolias [a]
[a] Department of Geology, University of Patras, GR-265 00, Patras, Greece

First published on: 03 June 2009

To cite this Article Koukouvelas, Ioannis K., Kokkalas, Sotirios and Xypolias, Paraskevas(2009) 'Surface deformation during the Mw 6.4 (8 June 2008) Movri Mountain earthquake in the Peloponnese, and its implications for the seismotectonics of western Greece', International Geology Review, 52: 2, 249 — 268, First published on: 03 June 2009 (iFirst)
To link to this Article: DOI: 10.1080/00206810802674329
URL: http://dx.doi.org/10.1080/00206810802674329

International Geology Review
Vol. 52, Nos. 2–3, February–March 2010, 249–268

Taylor & Francis
Taylor & Francis Group

Surface deformation during the Mw 6.4 (8 June 2008) Movri Mountain earthquake in the Peloponnese, and its implications for the seismotectonics of western Greece

Ioannis K. Koukouvelas*, Sotirios Kokkalas and Paraskevas Xypolias

Department of Geology, University of Patras, GR-265 00, Patras, Greece

(*Accepted 14 November 2008*)

The Movri Mountain earthquake (Mw 6.4), western Greece, was likely caused by dextral-slip along a blind high-angle fault, and generated a complex pattern of co-seismic surface ruptures southwest of the Gulf of Corinth. The mapped Nisi, Michoi, and Vithoulkas rupture segments have similar lengths (5–6 km) and vertical offset on the order of 25, 10, and 5 cm, respectively. They are commonly expressed as straight or jagged linear traces with secondary cracks radiating from the main segments. Horizontal slip vector analysis indicates extensional faulting processes for all rupture segments. Although these faults exert some control on the fluvial drainage pattern and at least one of them was ruptured during past events, their escarpments are poorly preserved. The indistinct topographic expression of the studied faults and their complex rupture patterns can be attributed to the distribution of the deformation over a blind fault.

Keywords: surface ruptures; blind fault; diffuse deformation; strike-slip fault; Hellenic arc

Introduction

Shallow intra- and inter-plate earthquakes of moderate-to-large magnitudes often generate surface ruptures (Yeats *et al.* 1997). The co-seismic surface ruptures commonly follow a pre-existing fault but in some cases they have, in map view, a complex pattern making the correlation between ruptures and faults at depth a difficult task (Yeats *et al.* 1997; Lee *et al.* 2002; Bowman *et al.* 2003; Wen *et al.* 2008). Therefore, the study of co-seismic ruptures in terms of extent, style, geometry, and slip distribution is essential for understanding rupture behaviour, as well as for assessing future seismic potential (Sieh 1996; Yeats *et al.* 1997; Pavlides and Caputo 2004).

The dynamics of plate boundaries and, in particular, the interaction between subduction and mountain belt formation remains an open problem in tectonics. Western Greece is one of the places on Earth where such a process can currently be observed. The area is characterized by high seismicity and a fairly complex three-dimensional geological setting, with along strike changes in the subduction zone geometry and dynamics and the rock units involved, comprising continent–continent subduction (collision) in the north and ocean–continent subduction in the south (Underhill 1989; Hatzfeld *et al.* 1990, 1995; Hirn *et al.* 1996; Sachpazi *et al.* 2000; Doutsos *et al.* 2006). The change between continent-continent and ocean-continent

*Corresponding author. Email: iannis@upatras.gr

ISSN 0020-6814 print/ISSN 1938-2839 online

DOI: 10.1080/00206810802674329
http://www.informaworld.com

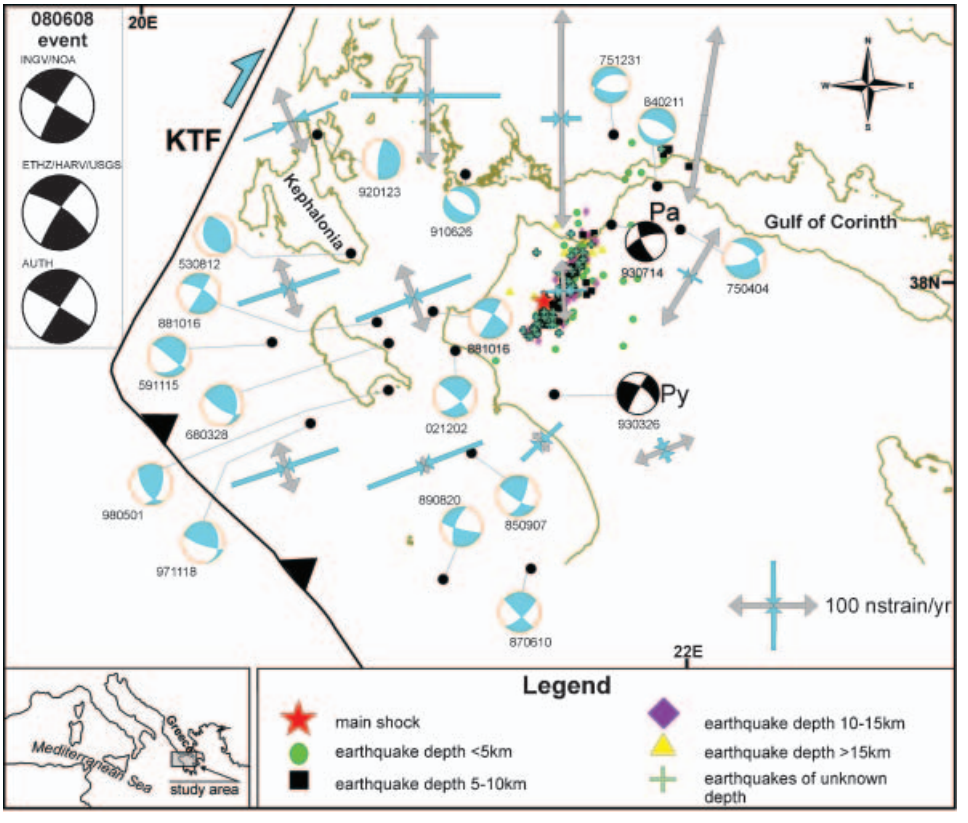

Figure 1. Structural map of the NW Peloponnese and the Ionian Islands showing published focal mechanisms of previous earthquakes, strain rates, and the aftershock cluster of the 8 June 2008 Movri Mountain earthquake. Inset shows the study area within the Mediterranean Sea. Focal mechanisms and epicenters of selected earthquakes compiled from: Hatzfeld *et al.* (1995); Koukouvelas *et al.* (1996); Sachpazi *et al.* (2000); Tselentis (1998); Roumelioti *et al.* (2004). Aftershock epicentres are from the National Observatory of Athens (http://www.gein.noa.gr). Principle axes and eigenvalues showing strain rate results for the study area (grey arrows indicate extension, and light-blue arrows compression) after Hollenstein *et al.* (2008). These strain rate results show compression perpendicular to the Hellenic arc, dextral shear strain rates along the KTF resuming into extension across most of the faults on the Peloponnese and the Gulf of Corinth (for more details see Hollenstein *et al.* 2008).

subduction occurs at the Kephalonia transform fault (KTF; Figure 1) (Kokkalas *et al.* 2006), which is characterized by a dextral strike-slip sense of shear.

GPS data from the Dalmatian-Albanian coastal region and northwestern Greece indicate a belt affected by NE–SW shortening. GPS strain rates within this area are low, whereas focal mechanisms of moderate to strong shallow earthquakes indicate prominent thrust faulting (Mantovani *et al.* 1992), which is possibly associated with the collision of the Adriatic block with the Eurasia plate. GPS data from western Greece show a small amount of motion north of the KTF and southwest-directed rapid motion of the overriding plate south of it that reaches rates of 30–35 mm/yr in the western parts of the Peloponnese along with dextral kinematics (Lagios *et al.* 2007; Hollenstein *et al.* 2008). Particularly along the area of KTF, strong earthquakes ($M>6.3$) are common (Hatzfeld *et al.* 1995; Roumelioti *et al.* 2004).

Well-constrained focal mechanism solutions exhibiting reverse-faulting striking NW–SE have been reported for a number of earthquake events located under the Ionian Islands, such as the Kephalonia earthquake (12 August 1953) of M=7.4 (Sachpazi *et al.* 2000; Figure 1). The focal depths of all recorded reverse faulting events are not well constrained but some of them are placed just above the plate interface, implying internal deformation in the overriding plate. Field observations made after the Lefkada earthquake of Ms=6.4 (14 August 2003) at a depth of 15 km, also showed indications of recent reactivation along NNE–SSW-striking faults, with sinistral sense of motion, trending parallel to the Ionian thrust (Kokkalas *et al.* 2003; Figure 2).

East of the Ionian Islands, all types of focal mechanisms characterize the seismicity at various depths; however, this seismicity resumes in the Greek mainland with primarily normal fault mechanisms (Sachpazi *et al.* 2000; Figure 1). The Ionian Channel, which occupies the area between the Ionian Islands and the Greek mainland, has been noted, in temporary deployments of high accuracy seismic networks, to have reduced seismic activity. However, up to now it remains

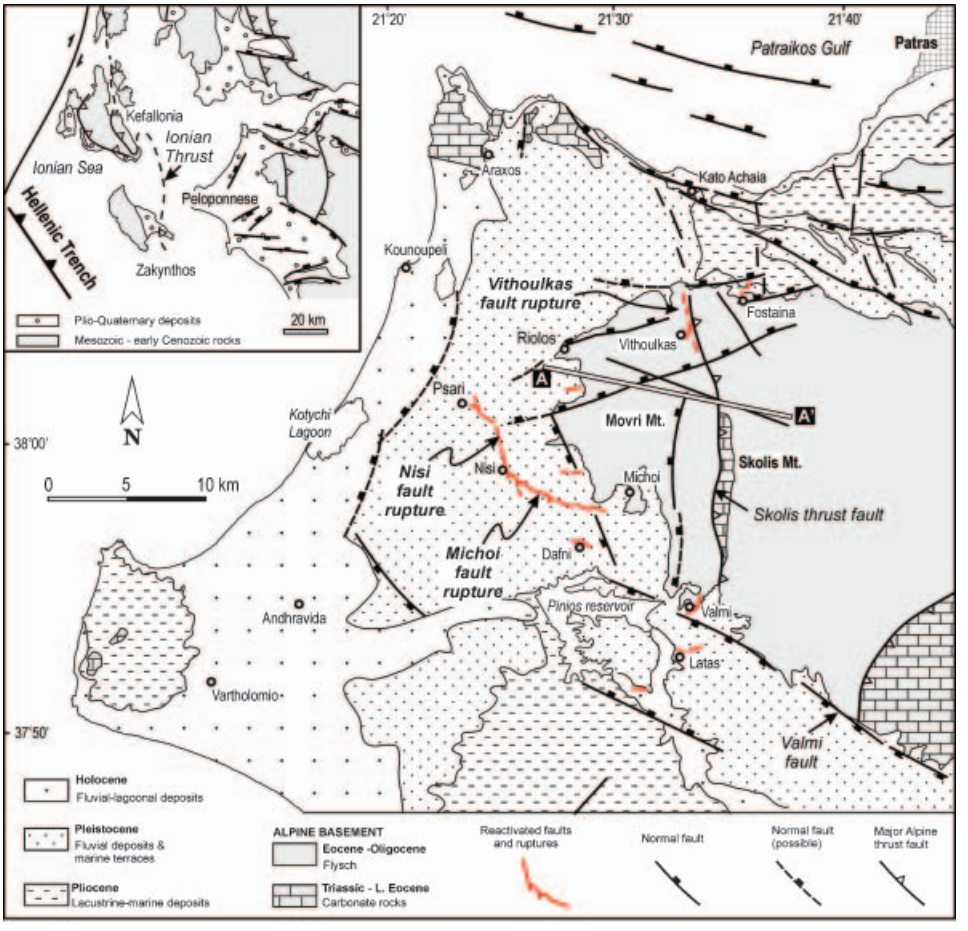

Figure 2. Geological map of the NW Peloponnese showing active faults in the Dafni Basin and the reactivated faults during the 2008 Movri Mountain earthquake. The map is compiled from Zelilidis *et al.* (1988); Kamberis *et al.* (2000, 2005).

controversial whether this is the case for a long period or is the result of short period deployment (Sachpazi *et al.* 2000).

Destructive earthquakes in the NW Peloponnese

The NW Peloponnese is the locus of a series of destructive earthquakes that display similar strike-slip focal mechanism solutions and nodal plane orientations. Here, we focus attention on earthquake events during the last 30 years because these events are generally well constrained in terms of their epicentre, depth, and focal mechanism. All these events caused primarily damage to buildings and to a lesser extent human loss or injuries. Among these events, the 2008 Movri Mountain earthquake (Mw=6.4) was the most destructive over this period, affecting the whole NW Peloponnese and causing serious ground hazards and extensive damage to buildings along a 30 km long and 20 km wide area parallel to the Ionian Sea coast. The main shock that occurred on 8 June 2008 (UTC 12:25:28.0), recorded by the seismic network of the National Observatory of Athens, was located at latitude 37.98°N and longitude 21.51°E (http://www.gein.noa.gr/index-en.htm). The main event was followed by a series of aftershocks with maximum magnitude of 5.1 (Figure 1). Although all reported focal mechanisms of the 2008 Movri Mountain event indicate almost pure strike-slip kinematics, significantly different estimations of the focal depth and exact location of the epicentre were reported. Regarding the focal depth, estimations vary from 5 to 30 km, while for the epicentre location several calculations place the main event either west or east or south of the N–S trending Skolis Mountain. Even with these uncertainties in the depth or the location of the reported epicentre, the consistency of the focal mechanism suggests that the 8 June 2008 event belongs to a series of earthquakes that show strike-slip focal mechanism solutions that operated in the area between Zakynthos Island and Patras town (Figure 1). Most of these events were moderate in magnitude ($4.7<Mw<6$), with their epicentral areas either small or offshore, and consequently damage was limited.

The first earthquake of this series, on 16 October 1988 (Mw=5.9), was an offshore event (Figure 1, event 881016) that caused limited destruction to buildings of Vartholomio town (Lekkas *et al.* 1990; Papadopoulos and Profis 1990; Papadopoulos and Plessa 2000). After this event, the 26 March 1993 (Mw=5.5) onshore Pyrgos earthquake (Figure 1, event 930326) caused significant damage to buildings of Pyrgos town and triggered a series of landslides and liquefactions around it (Koukouvelas *et al.* 1996). In the same year, Patras town experienced a moderate magnitude earthquake (Mw=5.4; Tselentis 1998) on 14 July 1993 (Figure 1, event 930714). These two events attracted the interest of the scientific community because they caused significant damage to buildings and were difficult to understand in terms of the surface traces of active faults in the NW Peloponnese. In this region, structural mapping shows that most of the active faults are oriented WNW–ESE (Koukouvelas *et al.* 1996; Zelidis *et al.* 1988); but the focal plane solutions suggest activity along NW–SE-trending faults (Tselentis 1998). The series of these moderate-in-magnitude events were followed by the 2 December 2002 Vartholomio (M=5.5) on the Kyllini Peninsula, and the 4 February 2008 Chalandritsa (Mw=4.8) earthquakes (Figure 1, events 021202 and 080204) (Sachpazi *et al.* 2000; Roumelioti *et al.* 2004; EMSC 2008: http://www.emsc-csem.org/index.php?page=home). Unfortunately, none of these moderate events produced surface ruptures, hence the nature of seismic deformation at depth

and the surface deformation remain controversial (see also discussion in Koukouvelas *et al.* 1996).

Nevertheless, these earthquakes bring up for discussion quite an important question of whether these events were hosted on blind faults or whether structural mapping in the NW Peloponnese has failed to recognize a series of almost N–S trending strike-slip faults (Figures 1 and 2). The recent Movri Mountain earthquake is a strong event showing strike-slip kinematics at depth, characterized by extensive but rather complex surface rupture patterns, offering a rare opportunity to describe for the first time surface deformation in an area of limited outcrop and to correlate deformation processes at depth with those at the surface (Kokkalas *et al.* 2008).

In this paper we present a natural example of complex co-seismic surface ruptures generated by the 8 June 2008 earthquake swarm (Mw=6.4), and we investigate the relation between seismogenic sources and mapped faults at the surface. We describe in detail the characteristics of the surface rupture segments, as well as kinematic analysis of the surface faulting based on outcrop measurement in the field, and try correlating these surface ruptures with the geological evolution of the Pliocene-Pleistocene Dafni Basin. Our work attempts to shed light on the following questions. (1) Are the surface ruptures of tectonic origin? (2) Is the main fault, which ruptured at depth blind, or it has a surface expression? (3) How does the surface deformation resemble the deformation at depth? And (4) were these complex earthquake surface ruptures guided by specific local geological features?

Tectonic setting

The NW Peloponnese has a complex geologic history of tectonics and erosion. However, the active deformation in western Greece could be described in spatiotemporal continuation with the foreland-propagated fold-and-thrust belt of the External Hellenides, which can be followed along the Hellenic arc (e.g. Underhill 1989; Doutsos *et al.* 2006). In detail, during the Eocene, the Peloponnese was characterized by an Alpine collisional history, which led to the assemblage of intra-Tethyan continental fragments (e.g. Apulia and Pelagonian microcontinents) and the formation of the Hellenic mountain range (Doutsos *et al.* 1993, 1994; Dilek *et al.* 2007). Mesozoic–early Cenozoic carbonate rocks originally deposited on a series of platforms (pre-Apulian and Gavrovo zones) and basins (Ionian and Pindos zones) were telescoped along N–S striking and east-dipping thrust faults that propagated upward and westward into overlying flysch deposits (Fleury 1980; Xypolias and Doutsos 2000; Skourlis and Doutsos 2003; Sotiropoulos *et al.* 2003). The latter are represented by upper Eocene to upper Oligocene turbiditic and hemipelagic sedimentary rocks deposited in foredeep and/or piggyback basins that evolved during thrust sheet emplacement (Kamberis *et al.* 2005; Xypolias and Koukouvelas 2005; Doutsos *et al.* 2006). These flysch deposits constitute the basement of the Dafni Basin.

From the late Miocene onwards, thrust faulting progressively shifted westward from the Peloponnese area to the Ionian Sea (Doutsos *et al.* 1987, 1988; Underhill 1989). late Miocene-Quaternary compressional structures have been recognized on the Ionian Islands from field-based studies, as well as from deep seismic profiles (Doutsos *et al.* 1987; Underhill 1989; Kamberis *et al.* 1996). Of particular interest, both on the Ionian Islands and on the mainland Greece, are the Triassic evaporitic layers that overthrust Pliocene sedimentary rocks along the Ionian thrust in both the offshore area between Zakynthos Island and within the upper part of the crust of the

Peloponnese (Monopolis and Bruneton 1982; Underhill 1989; Kamberis *et al.* 2000). The lower Miocene-Quaternary sedimentary succession extends over most of the area in the Ionian Channel and progressively thins eastwards (Monopolis and Bruneton 1982).

An extensional stress field has prevailed in the northwestern Peloponnese from the early Pliocene up to the present, generating two major sets of active normal faults with NE–SW and WNW–ESE trends, respectively (Figure 2; Doutsos *et al.* 1988; Koukouvelas *et al.* 1996; Doutsos and Kokkalas 2001). From a geodynamic point of view, the synchronicity of these differing styles of post-Miocene deformation in the frontal and inner parts of the overriding plate of the modern Hellenic subduction zone possibly reflects diffuse deformation caused both by rollback of the subducting slab and by the propagating North Anatolian fault (Doutsos and Kokkalas 2001; Kokkalas *et al.* 2006). The complexity of the structure in the westernmost end of the Hellenic subduction is reflected in the great variety of earthquake focal mechanisms.

Dafni Basin evolution

Lower Pliocene-Holocene sediments infilling extensional basins are well represented throughout the northwestern Peloponnese (Figure 2). As revealed by litho- (Hageman 1976; Zelilidis *et al.* 1988) and chrono-stratigraphic studies (Frydas 1987; Stamatopoulos *et al.* 1998), sedimentation started with the deposition of Pliocene lacustrine-marine sediments followed by Pleistocene terrestrial fluvial deposits and marine terraces. Holocene sediments are discernible in fluvio-lagoonal deposits traced along the western coastal zone (Figure 2). The distribution of sedimentary facies characterizing this succession together with evidence of syn-sedimentary activity along the major border faults indicate that NNE- to NE-trending normal faults accommodated most of the extension. Their development appears to have controlled the deposition of sediments ranging from lower Pliocene to Holocene (Doutsos and Poulimenos 1992; Koukouvelas *et al.* 1996). The second major set of WNW-striking normal faults is associated with Pleistocene to Holocene sediment accumulation and appears to accommodate a smaller amount of the regional extension, as indicated by slightly rotated beds and small displacements (up to 500 m) occurring along these faults. This fault set produces some of the most outstanding morphotectonic features of the northwestern Peloponnese including river courses and shallow gulfs (e.g. Patraikos Gulf). However, both major sets of faults are active. Fault-slip analyses for the broader area of NW Peloponnese yield a stress tensor with the least compressional axis (σ_3) trending almost N–S, comparable to the state of stress recorded by GPS and seismicity data (Figure 1; Hirn *et al.* 1996; Sachpazi *et al.* 2000; Hollenstein *et al.* 2008).

Surface ruptures during the Movri Mountain earthquake

In the immediate aftermath of the Movri Mountain earthquake, attention was initially focused on a NE zone defined by the aftershock distribution (Figure 1) and finally covered almost all of the affected area (Figure 2). The field survey, which was carried out on the day after the earthquake and in the following two weeks, found no surface ruptures or evidence of activity along faults or morphotectonic features following this NE-trend, but only small-scale fissuring (e.g. Fostaina and Valmi villages, Figure 2). Field mapping of the fault surface ruptures during 8 June 2008, earthquake depicts a complicated pattern, comprizing three main segments called

hereafter Nisi (trending almost NNW–SSE), Vithoulkas (trending almost N–S), and Michoi (trending WNW–ESE) rupture segments (Figure 2). Surface ruptures are commonly expressed as either straight strands or jagged linear traces, with numerous secondary cracks radiating at fairly consistent angles from the main segments. Topographic and geometric features of ruptures are indicative of normal offset at the surface with components of strike-slip motion along certain rupture segment orientations. The surface ruptures were produced either on flysch deposits (i.e. the Vithoulkas segment) or in the Pleistocene fluvial deposits and marine terraces of the Dafni basin (i.e. the Nisi and Michoi segments). This kind of area is difficult to survey, inasmuch as most surface features of past earthquakes have been obscured by sedimentation – or cultivation – leaving no trace on the surface of any previous fault activity.

Survey methods and mapping of ruptures

Almost all the surface breaks we mapped were examined on foot for almost their entire length. Surface traces were extrapolated only in cases of inaccessible areas, such as steep slopes or highly vegetated areas. A Pro-Mark 3 Thales high accuracy (± 1 m real time accuracy) GPS-system was used to obtain accurate locations of the mapped faults and associated features (sand blows, ground fissures, landslides etc.) on the measurement sites.

Numerous types of features provided piercing points to measure vertical and lateral offsets. These included man-made features such as, roads, railway tracks, concrete pipes, as well as split cobbles, minor ridges, mud cracks, offset thalwegs of small gullies and pre-existing fractures.

Horizontal tensional direction was determined by matching faces on both sides of a rupture or restoring in places the deformed structures to their original forms prior to the earthquake event. In measuring offsets, preference was given to sites that had relatively simple surface rupture geometry and piercing points that we could confidently correlate across the fault. Minor deviation from even sampling along the surface ruptures was due to ground shattering, or non-tectonic slumping that obscured the rupture trace in some sections. Even so, there is an inherited uncertainty in the measurements that primarily reflects limited knowledge of the geometry of a feature prior to its fault offset.

Nisi rupture segment

The 6 km long Nisi rupture segment extends from Psari Village in the north to almost 1 km south of Nisi Village (Figures 2 and 3). These nearly continuous ruptures strike NNW (340°) across Pleistocene terrestrial deposits and locally a thin veneer of recent materials that blanket the alluvial deposits. To the south and north of the study area, no remarkable surface ruptures were developed, although small extensional features formed locally. Agricultural activities in the cultivated areas after the earthquake wiped out even small-scale fissures that might have been visible. In Nisi Village, an unambiguous surface rupture segment extending for almost 2 km (with strike 345–350°), cut across houses, vegetated fields and intervening footpaths, roads, and embankments, as well as on roadcuts showing clearly its connection to faulted sedimentary successions and the vertical component of motion on the surface. The surface rupture typically consists of en echelon breaks, 100 m in length, that in places step over to the left or right, producing small local domains of

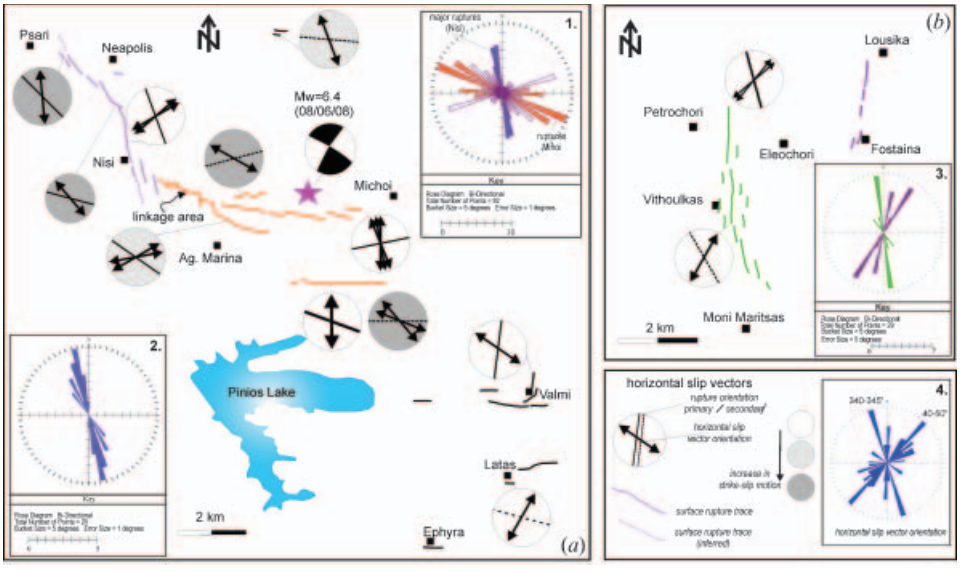

Figure 3. Maps showing the three rupture segments during the Movri Mountain earthquake. (a) Map showing geometric and kinematic data for the Nisi and Michoi ruptures. Rose diagram (1) shows variation in the orientation of surface ruptures for the Nisi segment as blue colour classes and for Michoi segment as orange colour classes. White colour classes correspond to orientation variation at the linkage area between the two rupture segments. Small circles represent the trend of horizontal slip vectors in relation to rupture orientation. Shading of circles corresponds to the increase in strike-slip motion. (b) Map showing geometric and kinematic data for the Vithoulkas rupture segment. Rose diagram (3) shows variation in the orientation of surface ruptures in green and purple near the Vithoulkas and Fostaina Villages, respectively. Rose diagram (4) summarizes variation in horizontal slip vectors orientations.

extension or shortening. Some of the rupture segments, particularly those associated with larger amounts of surface slip, exhibit continuous breaks for hundreds of metres. Detailed mapping demonstrates, however, that the surface rupture is highly sinuous in the smaller scale, ranging from a NNW to a WNW orientation. The latter orientation shows an apparent sinistral motion, whereas in some sites it displays reverse movements, probably due to the complex local geometry of the fault strands.

For this reason, our mapping efforts were concentrated in the northern part of the Nisi rupture segment because it showed larger displacements, up to 25 cm, compared to all other examined segments. Here, the Nisi segment appears as a sub-vertical to steeply dipping (dip angles 75–80° to the west) NNW-trending fault with a significant normal slip component. It is locally segmented by secondary WNW-trending ruptures showing oblique left-lateral motion (Figures 4 and 5). The intersection between the NNW- and WNW-trending segments are locally very distinct, occur over lateral distances of as short as 10 m but also on a larger scale of 100 m, and display changes in strike between 40 and 50°. Within the step over zones, local changes in fault geometry result in the formation of both pressure ridges and small grabens (Figure 4(d)). Local strike, vertical throw, and heave (apparent horizontal component of net slip) were measured in approximately 26 sites along this rupture segment (Figure 5(b)). At this location, the fault trends N20°W with small deviations of 5–10° in strike and only toward its northern termination it displays a zigzag style of fracturing intersecting with small-scale N90°E striking

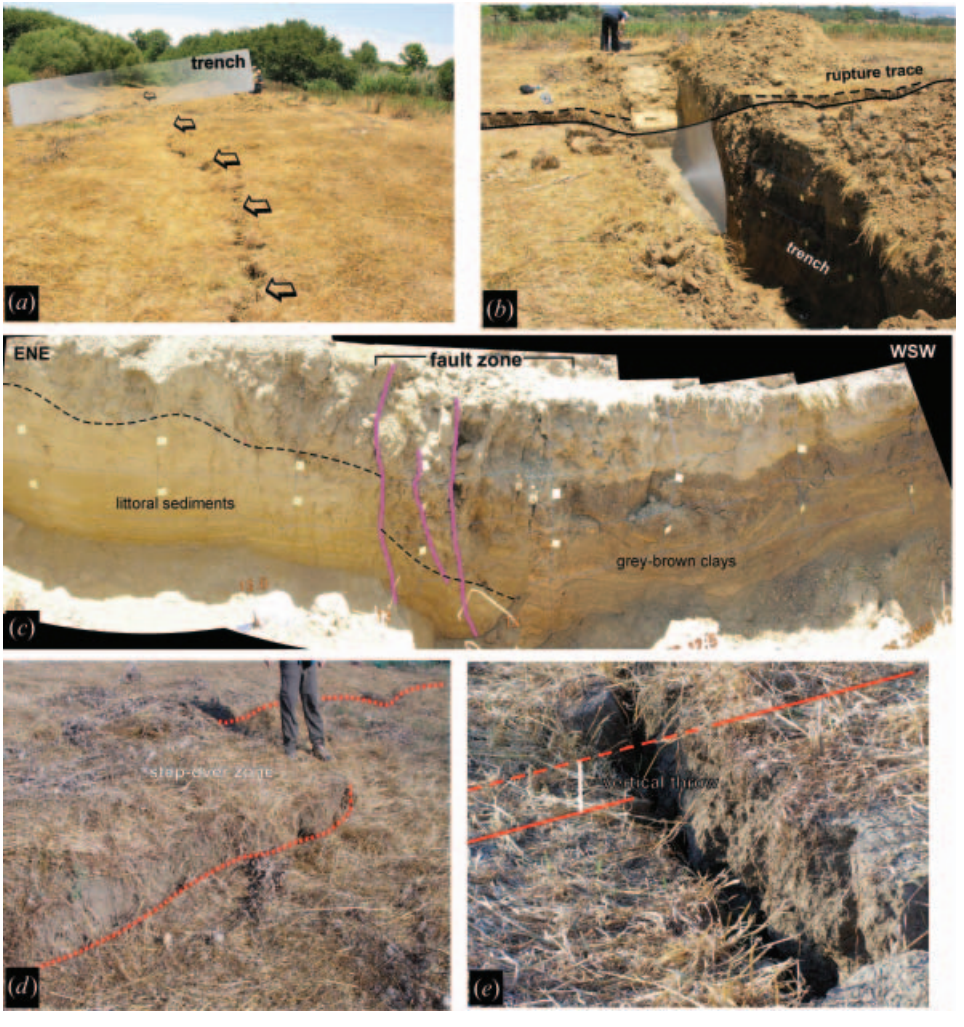

Figure 4. Details of the Nisi fault rupture. (a) Photo of the NNW-trending surface rupture showing also bulging of the footwall (right half of the photo) and warping of the hanging-wall block toward the fault plane. The position of the excavated trench is also shown. Photo was taken looking northwest. (b) General view of the palaeoseismological trench excavated across the Nisi fault. (c) Detailed view of the palaeoseismological trench after cleaning and gridding. Note the 1-m wide fault zone comprising several fault strands with some of them characterized by open voids, caused from the last earthquake event. The footwall of the fault occupies yellowish littoral sediments while the hanging wall comprises grey-brown clays. (d) Detailed view of the surface ruptures showing a step over zone. (e) Detail of the surface rupture showing 25 cm vertical throw (white bar) and 10 cm aperture.

segments. Significant vertical displacements, up to 25 cm (Figures 4 and 5(b)), have been identified along this high angle NNW-striking segment.

Distance versus vertical throw and heave diagrams from the northern part of the Nisi surface rupture, where the highest surface offset was recorded, depict segmentation of the surface rupture in four smaller scale sub-segments (Figure 5(b)). Vertical throw diminishes rapidly close to the tips of each segment, while in some cases it passes onto the next sub-segment with no significant decrease

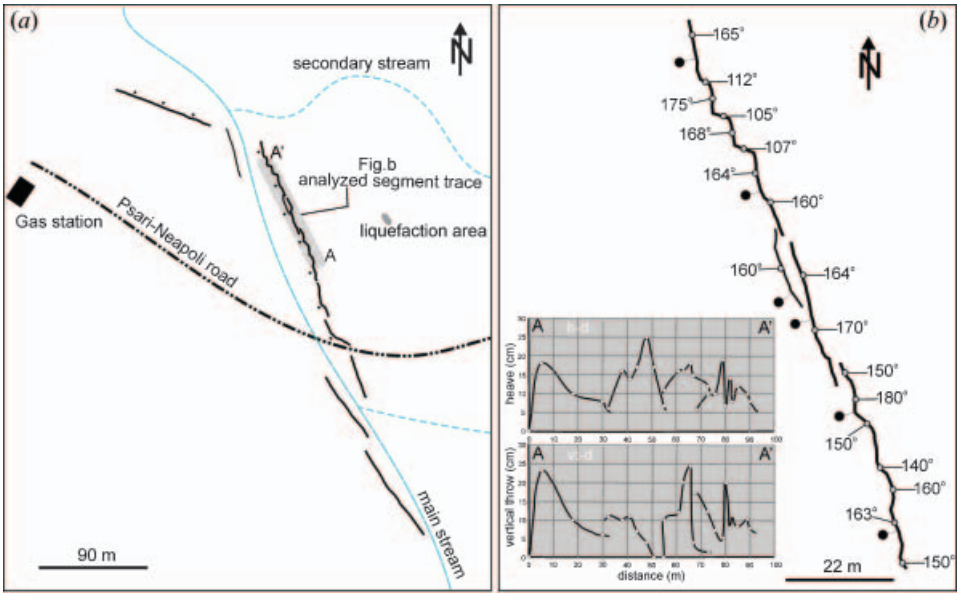

Figure 5. (a) Map of the north-westernmost end of the Nisi rupture. Grey shading denotes the detailed structural map of Figure 5(b). (b) Detailed structural map of the surface trace of the Nisi fault tip showing orientation complexity, segmentation, and step over geometry. The graphs show heave and vertical throw variation along-strike.

in displacement (Figure 5(b)). Fault dip changes along strike can cause a poor correlation between horizontal heave and vertical displacement, as observed in the graphs. In the northernmost sub-segment, the great variation in both heave and vertical throw values within a short distance is caused by the zigzag style of rupture propagation. Even in places where the rupture is roughly straight and has consistent slip azimuths, vertical throw and heave oscillate rather smoothly in a cm to meter distance along the rupture trace (Figure 5(b)).

Another surprising result is that the Nisi rupture segment, which accommodated the highest displacement compared to all other ruptures in the area, did not occur on a previously mapped basin-bounding fault with a visible surface trace; it occurred in a flat area parallel to the basin's faulted margin farther west where a striking change from E–W to NW–SE in the river drainage pattern is evident. In order to investigate whether this rupture and associated fractures record an incipient tectonic surface offset or a response to strong ground motion, we excavated a palaeoseismological trench across the surface rupture trace (Figure 4(a)–(c)). The trench revealed a ~1 m-wide-fault zone with several west-facing steeply-dipping fault strands. The footwall block comprises yellowish littoral sediments whereas the hanging-wall comprises a dark brown-grey silt and gravel sequence (Figure 4(b) and (c)). Close to the fault zone, the strata in the hanging-wall are highly rotated, whereas 2 m away they remain horizontal up to the end of the excavated trench. Inside the fault zone, at least two previous earthquake events were identified. A key element, for dating these features, is that the littoral sediments in the footwall block have been dated around 100 ka based on $^{230}Th/^{238}U$ radiometric dating of corals (Cladocora sp.; Stamatopoulos *et al.* 1998). Finally, based on the palaeoseismological section we interpret this surface feature as a previously unmapped fault. We call this fault the Nisi fault.

Michoi rupture segment

The Michoi segment represents a ~5-km-long, WNW-trending zone of ruptures occupying the broader main shock epicentral area (EMSC epicentre) between Nisi and Michoi villages (Figure 3). Close to the western end of the zone and towards the southern termination of the Nisi rupture segment, the surface ruptures gradually turn from a NNW–SSE to a more-or-less WNW–ESE orientation, forming several discontinuous sub-segments distributed within a 1-km-wide area (Figure 3). More specifically, in this area we mapped a series of both right and left stepping segments (Figure 3) with a WNW trend that intersect with NNW- to NW-striking segments at high angles.

A simpler pattern of ruptures was mapped in the central and eastern part of the zone between Ag. Marina and Michoi villages (Figure 3). This zone has an almost E–W strike, comprising en-echelon fractures forming a 10-m-wide zone that appeared also in the nearby fields (Figure 6(a) and (b)). Kinematic analysis in the zone showed mainly an oblique left-lateral normal component of motion (Figure 3(a)). Measurements along this segment showed values of vertical throw in the order of 10 cm and heave values ranging from 10 to 40 cm. The rupture zone lies on top of a ridge and parts of it also may be related to strong ground-shaking. However, because of its occurrence in the same geometric and kinematic style on the flat lying areas on either sides of the ridge, it is interpreted to have a tectonic origin (Figure 6(b)). Moreover, this rupture zone runs parallel to the drainage pattern in the area around the Michoi village and is also parallel to the Valmi fault to the south (Figure 2). Based on these observations, we conclude that the Michoi rupture segment possibly represents a reactivated fault herein recognized as the Michoi fault.

Vithoulkas rupture segment

The ~N–S trending and ~4.5-km-long, Vithoulkas rupture segment is the easternmost segment of the 8 June 2008 earthquake and extends from Moni Maritsas in the south to 1 km east of the Petrochori village to the north (Figures 3 and 7). Despite an intensive search for a continuation of surface rupture to the north, a gap with no discernible surface rupture separates the area between Petrochori and Kato Achaia. In the latter area only some isolated ruptures close to the railway tracks were identified. Therefore, it seems that the rupture has jumped farther east, where another 2.5-km-long rupture segment of the same strike extends from Fostaina to Lousika Village (Figures 3 and 7(d)).

The N–S to NNE–SSW trending rupture zone in the Vithoulkas-Petrochori area (Figures 3 and 7(a)) was mainly measured along a ~500-m-wide zone of distributed surface cracking and diffused deformation, accompanied by many minor rock falls and large landslides. This rupture segment, which aligns well with the up-to-now aftershock distribution, typically consists of en echelon left-stepping short segments (Figures 7(b) and (c)). Individual rupture segments extended for a few hundred metres to almost 2 km in length, and are commonly smooth and nearly planar in places. Close to step-over zones, the damage zone broadened and is more structurally complex, forming smaller overlapping segments or appears as a narrow mole-track a few metres wide. Individual cracks have displacements ranging from zero to 5 cm, whereas opening on fractures ranges from zero to 15 cm. In contrast to the Nisi and Michoi segments, the Vithoulkas rupture has significantly fewer steps

Figure 6. Key outcrops of the surface rupture along the Michoi fault. (a) A 3-m-wide zone of surface ruptures mapped on 11 June 2008, showing step-type geometry of faulting in the north half of the photo and a graben in its central part. Photo is taken looking west, location 1 km south of the epicentre and west of Michoi village. (b) Helicopter view of the Michoi surface rupture 0.8 km west of Michoi village. (c) Detail of the WNW-trending surface rupture close to Dafni Village (for location see Figure 2).

and segments and extends more or less in a constant N–S orientation. Remarkably, this orientation lies parallel and close to the Skolis thrust fault (Figure 2). However, inasmuch as this rupture zone hosts a series of landslides and controls a steep valley along with the change in facies to the north of the mapped ruptures in the Patraikos Gulf onshore basin, we interpret it as an active fault (Figure 2).

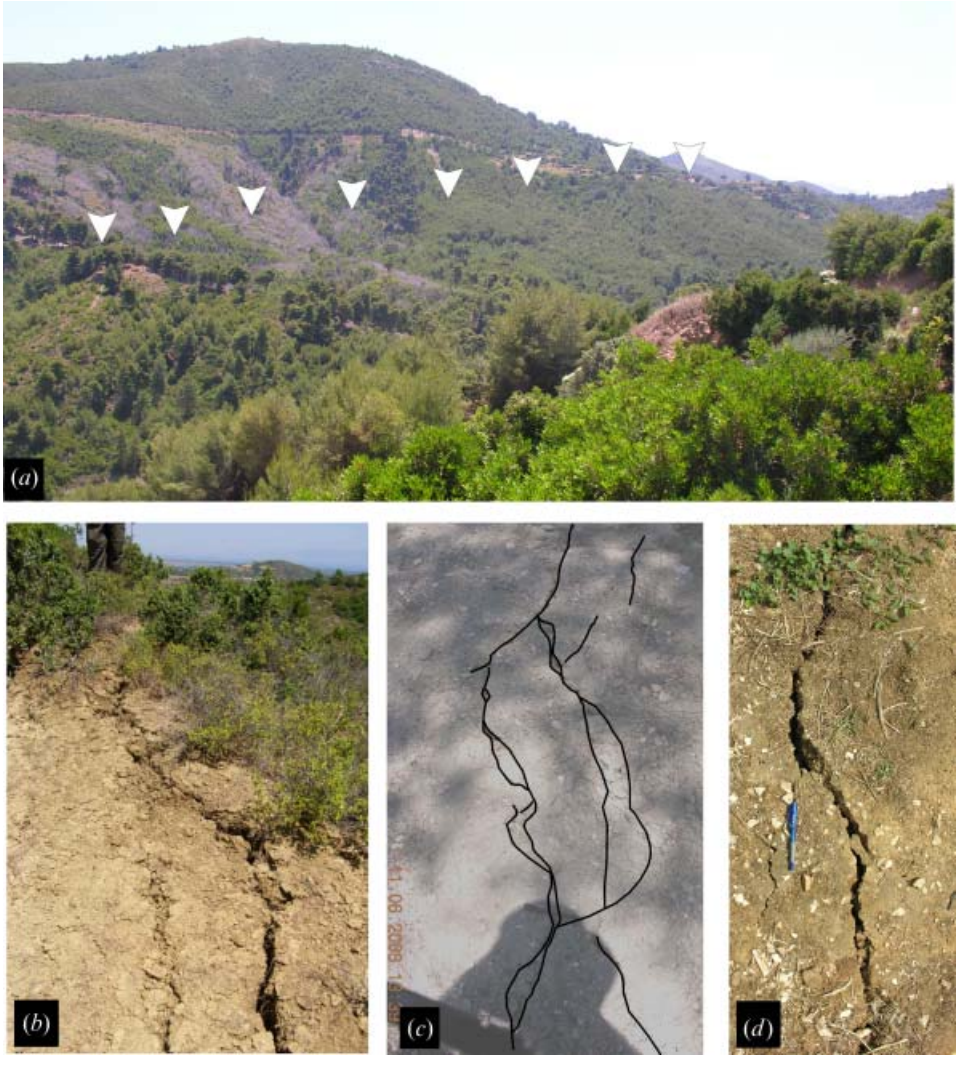

Figure 7. (a) The Vithoulkas fault denoted by change in the slope of the hill and, marked on the photo by a series of white arrowheads, opposite to the Vithoulkas village. Some triangular facets are developed in the footwall of the fault. Photo is taken looking SE. (b) Ruptures at the hilly area east of Vithoulkas village showing characteristic moletracks. Photo was taken looking north. (c) A typical step over zone developed between two surface ruptures in the Vithoulkas Valley. Photo is taken looking down. (d) A rupture just east of Fostaina village; photo is taken looking down.

Horizontal slip vectors

About 80 slip vector azimuths were measured, both on primary and secondary rupture sub-segment traces and are presented in Figure 3. Despite local variations, main slip azimuths are fairly consistent in two major orientations: (1) NE–SW orientation (35–55°) along the NW-striking Nisi rupture segment and the roughly N–S Vithoulkas rupture segment; and (2) NNW–SSE trending (340–350°) along the ENE- and WNW-striking segments of the Michoi rupture zone. The measured slip

azimuths can vary locally over 50° where rupture is irregular or associated with flexure or subsidence in overlap or step-over zones.

The NW-slip, as well as the secondary WNW-directed slip, measured along the Nisi rupture also resulted in significant left-lateral oblique motions along the WNW and NW-striking sub-segments, respectively. Correlation of these motion vectors with syn-earthquake surface motion data from onsite GPS surveys (not released yet) would provide a better insight and understanding about deformation and how the fault block moved or rotated at the surface.

Discussion

Fault patterns and subsequent strain variation in areas located along plate margins or within crustal parts with inherited anisotropy indicate that the role of pre-existing structures is quite critical in the active tectonic deformation within the overriding plate (Rebai *et al.* 1992; Sassi and Faure 1996; Andeweg *et al.* 1999; Tikoff and Wojtal 1999; Bowman *et al.* 2003; Kokkalas *et al.* 2006). In the area between the Ionian Islands and mainland Greece, a transition from E–W shortening to extension occurs, from west to east (Kokkalas *et al.* 2006; Hollenstein *et al.* 2008). Within this structural setting, the 2008 Movri Mountain earthquake, located in this transitional area, also attests to the structural complexity.

Significance of the surface ruptures

Our field survey carried out in the period after the earthquake revealed three major surface rupture segments in the Dafni Basin. From a hierarchical point of view and in a descending structural significance documented by their length, displacement and the comparison with the already known structural pattern, these structures are the Nisi, Michoi, and Vithoulkas rupture segments, which are considered as active faults. Although the Nisi and Michoi fault segments were not previously mapped, strong evidence exists that both are active faults. Analytically, the mapped surface ruptures are of tectonic origin for the following reasons:

(1) Two of them (Nisi and Vithoulkas rupture segments) are compatible with the cloud of aftershocks (Figures 1 and 2).

(2) The trend of all mapped ruptures is parallel to the fault-controlled boundaries of the Dafni Basin, as well as to major fault sets (Figure 2). In detail, the WNW-trending Michoi fault rupture is parallel to the Valmi fault, which controls the southern end of the basin. The NNW-trending Nisi fault runs parallel to the Dafni Basin-bounding fault cropping out west of Michoi village (Figure 2). Note that the exposed lithologies in the area are highly eroded and fault scarps are not preserved, similar to the poor preservation of WNW-trending scarps in the Pyrgos Basin farther to the south (see also Koukouvelas *et al.* 1996). The Vithoulkas fault is parallel to a highly segmented fault that separates Pleistocene fluvial sediments in the west from Pliocene lacustrine-marine deposits in the east (Figure 2; Zelilidis *et al.* 1988).

(3) In all surface rupture cases, we have interpreted only those that have length longer than 200 m as co-seismic. These individual surface ruptures within fault segments are parallel to each other and in map view display a well-defined alignment. Moreover, slip distribution and estimates of both surface offset and fault rupture length, in combination with the seismic magnitude

of the earthquake, are in good agreement with many published geological data (e.g. Ferrill *et al.* 2008).

(4) The NNW-trending Nisi fault controls a series of third-order channels and the Kladeos River that drains a significant part of the Dafni Basin. In addition the overall drainage pattern in the area between the Riolos Village to the north and the Dafni Village to the south is characterized by a zigzag pattern. This drainage pattern is defined by WNW- and NNW-trending gorges parallel to the surface expression of the Nisi and Michoi fault ruptures. Because these rivers are of the Schumm's alluvial types and these are by definition quite sensitive to tectonic movements over several places in the Peloponnese (e.g. Koukouvelas 1998), we suggest that the drainage is completely fault controlled and the two faults remain active. Moreover, the WNW-trending faults seem to play a significant role in the recent evolution of the entire NW-Peloponnese, inasmuch as they control the recent drainage pattern and the sedimentation of the lagoonal areas, as well as the Patraikos Gulf.

(5) All major co-seismic surface ruptures reported here were identified at sites where the water table is located at a depth of >10 m. This fact diminishes significantly the possibility that surface ruptures are due to lateral spreading or liquefaction phenomena.

(6) Anomalous spring recharge and reduction of productivity of the water wells or boreholes are related to the Nisi fault, attesting to its reactivation during the Movri Mountain earthquake. A remarkable example is the Kounoupeli spa spring, located along the NNW prolongation of the Nisi fault (Figure 2), which remained dry for the last 20 years, since a previous earthquake event, and was activated again after the Movri earthquake with 60 m^3/h artesian recorded discharges. The Nisi surface rupture in this area shows absence of surface expression cutting across a featureless plain made up of loosely consolidated sediments and cultivated areas.

Seismotectonics

All preliminary focal mechanisms of the main shock in combination with the surface distribution of aftershocks imply rupture of an N35°E-striking dextral strike-slip fault at depth (Figure 1). However, even if we assume that lithological complexities of the crustal structure have significantly affected the horizontal co-seismic displacement at the surface (e.g. Megna *et al.* 2008), none of the major surface fault ruptures described here can fit with a NE-trending fault at depth. The only exception to this geometry includes the NNE-striking surface ruptures recognized in the area between the Fostaina and Lousika villages (Figures 2 and 3). Moreover, our detailed structural survey enables us to state clearly that there is no evidence of reactivation along NE-striking normal faults in the area (Figure 3). The same conclusion can also be drawn for the major east-dipping thrust faults, such as the Skolis thrust, showing a typical ramp-flat-geometry at depth and an overall low-angle geometry (e.g. Xypolias and Doutsos 2000; Skourlis and Doutsos 2003; Doutsos *et al.* 2006). Thus, we conclude that the seismogenic fault at depth had no direct surface expression. Based on these results, we think that the possible candidate fault to cause this earthquake is a N–S trending high-angle fault, such as the one mapped by the seismic profiles underneath the Skolis Mountain (Figure 8;

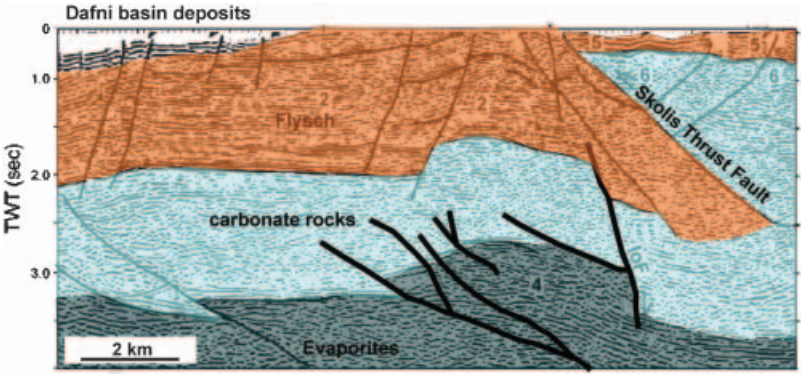

Figure 8. Interpreted seismic profile A–A' across the border of the Dafni Basin showing a buried flower structure at depth. Note that the flower structure is located in the area where the aftershocks are concentrated. The litho-seismic units and the faults are interpreted by Kamberis *et al.* (2005). For location of seismic line, see Figure 2.

Kamberis *et al.* 2000, 2005). A similar crustal scale structure has been also mapped by seismic reflection profiles in the area north of the Patraikos Gulf (Sotiropoulos *et al.* 2003). In the case of crustal section beneath the Skolis Mountain, a positive flower structure can be observed characterizing the upper tip zone of a possible strike-slip fault (Figure 8).

The aforementioned findings pose a serious problem for correlating normal faulting at the surface with strike-slip faults at depth. A possible solution is given by the slip partitioning model of Bowman *et al.* (2003), who showed that, depending on the relative strike-slip component and the dip of a blind fault, a zone of normal faulting can develop at the surface (Figure 9). This is because the upward crack propagation is controlled by the complex strain field around the tip of a blind fault, distributing deformation over several rupture planes with different orientations. The location and orientation of the new ruptures/fractures is influenced by pre-existing structures, as exactly describes the formation of all recognized fault ruptures in the study area. This style of diffused deformation probably explains why over past events, a complex pattern of rupture process affects the surface (Figure 9). In this way, active faults in the study area cannot build up significant offset in order to maintain a typical scarp morphology, in contrast to the well expressed fault scarps within the Gulf of Corinth (Zygouri *et al.* 2008).

Conclusions

(1) Three rupture segments with NNW–SSE, WNW–ENE and NNE–SSW trends were generated during the Movri Mountain earthquake event. These ruptures are located along three faults that show poorly preserved scarp morphology, but they control drainage patterns and basin boundaries. At least one of them, the Nisi fault, has been ruptured during past earthquakes. All these observations show that the Nisi, Michoi, and Vithoulkas are active faults.

(2) Eighty horizontal slip vector measurements are fairly consistent in NE–SW orientation (35–55°) along the Nisi and the Vithoulkas rupture segments and NNW–SSE trending (340–350°) along the Michoi rupture segment.

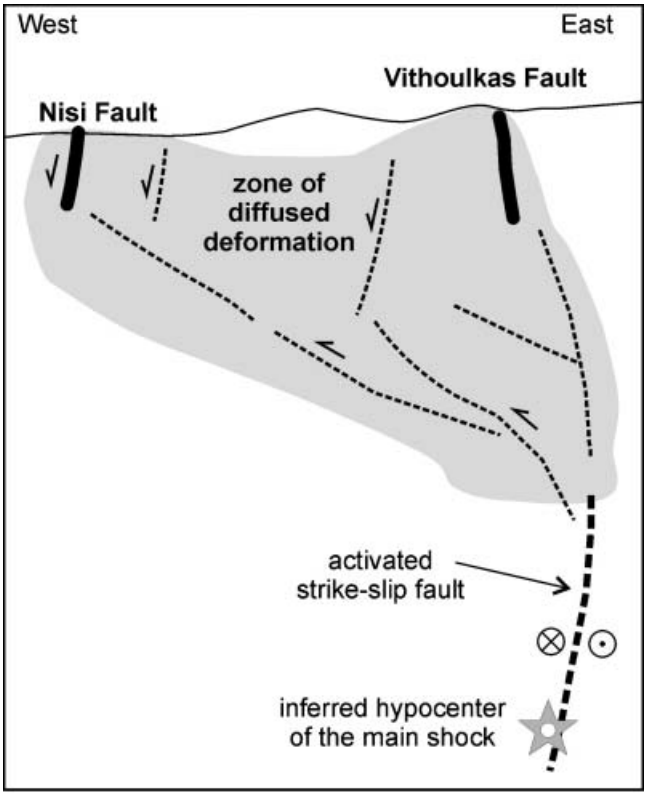

Figure 9. Schematic representation of the slip partitioning model applied for understanding the deformation during the 8 June 2008 Movri Mountain earthquake. The model shows a blind strike-slip fault at depth causing the formation of a positive flower structure at its tip, and the distribution of deformation near the surface.

These slip azimuths suggest primarily extensional deformation with a less important strike-slip component on the ruptured fault segments.

(3) The Nisi, Michoi, and Vithoulkas faults appear to accommodate extensional deformation in the upper crust over a buried strike-slip fault, suggesting that a mechanism of slip partitioning can be proposed to explain fairly well the spatial distribution of ruptured faults, their complex patterns and the absence of fault scarps.

(4) Active normal faults of the Corinth Gulf-type characterized by impressive scarps are missing in the Dafni Basin, because earthquake-related deformation at depth appears to be partitioned into several faults.

Acknowledgements

We would like to express our appreciation to S. Pavlides, R. Caputo, G. Papadopoulos, A. Chatzipetros, and A. Ganas, for fruitful discussion in the field, E. Kamperis for incisive discussion on the seismic line and E. Sokos for discussing seismological data. Thanks also are due to V. Zygouri, S. Verroios, V. Chatzaras and G. Sourlas for their help during the fieldwork. We would like also to thank Y. Dilek for his encouragement to submit this work and for his editorial help.

References

Andeweg, B., De Vicente, G., Cloething, S., Giner, J., and Munoz Martin, A., 1999, Local stress fields and intraplate deformation of Iberia: Variations in spatial and temporal interplay of regional stress sources: Tectonophysics, v. 305, p. 153–164.

Bowman, D., King, G., and Tapponnier, P., 2003, Slip partitioning by elastoplastic propagation of oblique slip at depth: Science, v. 300, p. 1121–1123.

Dilek, Y., Furnes, H., and Shallo, M., 2007, Suprasubduction zone ophiolite formation along the periphery of Mesozoic Gondwana: Gondwana Research, v. 11, p. 453–475.

Doutsos, T., and Kokkalas, S., 2001, Stress and deformation patterns in the Aegean region: Journal of Structural Geology, v. 23, p. 455–472.

Doutsos, T., Kontopoulos, N., and Frydas, D., 1987, Neotectonic evolution of northwestern continental Greece: Geologische Rundschau, v. 76, p. 433–452.

Doutsos, T., Kontopoulos, N., and Poulimenos, G., 1988, The Corinth-Patras rift as the initial stage of continental fragmentation behind an active island arc (Greece): Basin Research, v. 1, p. 177–190.

Doutsos, T., Koukouvelas, I.K., and Xypolias, P., 2006, A new orogenic model for the External Hellenides, *in* Robertson, A.H.F., and Mountrakis, D., eds., Tectonic Development of the Eastern Mediterranean Region: Geological Society London Special Publication 260, p. 507–520.

Doutsos, T., Koukouvelas, I., Zelilidis, A., and Kontopoulos, N., 1994, Intracontinental wedging and postorogenic collapse in the Mesohellenic Trough: Geologische Rundshau, v. 83, p. 257–275.

Doutsos, T., Pe-Piper, G., Boronkay, K., and Koukouvelas, I., 1993, Kinematics of the Central Hellenides: Tectonics, v. 12, p. 936–953.

Doutsos, T., and Poulimenos, G., 1992, Geometry and kinematics of active faults and their seismotectonic significance in the western Corinth-Patras rift (Greece): Journal of Structural Geology, v. 14, p. 689–699.

Ferrill, D.A., Smart, K.J., and Necsoiu, M., 2008, Displacement-length scaling for single-event fault ruptures: insights from Newberry Springs Fault Zone and implications for fault zone structure, *in* Wibberley, C.A.J., Kurz, W., Imber, J., Holdsworth, R.E., and Collettini, C., eds., The Internal Structure of Fault Zones: Implications for Mechanical and Fluid-Flow Properties: Geological Society London Special Publications 299, p. 113–122.

Fleury, J.J., 1980, Les Zones de Gavrovo-Tripolitza et du Pinde-Olonos; Evolution d'un Bassin dans leur Cadre Alpin: Societe Geologique du Nord, v. 1, no. 4, 651 p.

Frydas, D., 1987, Kalkiges Nannoplankton aus dem Neogen von NW-Peloponnes: Neus Jahrbuch fur Geologie und Palaontologie Monatshefte, v. 5, p. 274–286.

Hageman, J., 1976, Stratigraphy and sedimentary history of theUpper Cenozoic of the Pyrgos-area (Western-Peloponnesus), Greece: Annales Geologiques des pays Helleniques, v. 28, p. 299–333.

Hatzfeld, D., Kassaras, I., Panagiotopoulos, D., Amorese, D., Makropoulos, K., Karakaisis, G., and Coutant, O., 1995, Microseismicity and strain pattern in northwestern Greece: Tectonics, v. 14, p. 773–785.

Hatzfeld, D., Pedotti, G., Hatzidimitriou, P., and Makropoulos, K., 1990, The strain pattern in the western Hellenic arc deduced from a microearthquake survey: Geophysical Journal International, v. 101, p. 181–202.

Hirn, A., Sachpazi, M., Siliqi, R., McBride, J., Marnelis, F., and Cernobori, L., the STREAMERS–PROFILES Group, 1996, A traverse of the Ionian Islands front with coincident normal incidence and wide-angle seismics: Tectonophysics, v. 264, p. 35–49.

Hollenstein, Ch., Müller, M.D., Geiger, A., and Kahle, H.-G., 2008, Crustal motion and deformation in Greece from a decade of GPS measurements, 1993–2003: Tectonophysics, v. 449, p. 17–40.

Kamberis, E., Marnellis, F., Loukoyannakis, M., Maltezou, F., and Hirn, A., Streamers Group, 1996, Structure and deformation of the external Hellenides based on seismic

data from offshore western Greece, *in* Wessely, G., and Liebl, W., eds., Oil and gas in Alpidic thrust belts and basins of Central and Eastern Europe. European Association of Geoscientists and Engineer, Spec. Publ. 5: London, Geological Society, p. 207–214.

Kamberis, E., Pavlopoulos, A., Tsaila-Monopoli, S., Sotiropoulos, S., and Ioakim, C., 2005, Deep-water sedimentation and paleogeography of foreland basins in the NW Peloponnese (Greece): Geologica Carpathica, v. 56, p. 503–515.

Kamberis, E., Sotiropoulos, S., Aximniotou, O., Tsaila-Monopoli, S., and Ioakim, C., 2000, Late Cenozoicd eformationo f the Gavrovo and Ionian zonesi n NW Peloponnesos (Western Greece): Annali di Geofisica, v. 43, p. 905–919.

Kokkalas, S., Koukouvelas, I., and Doutsos, T., 2003, Relationship between tectonic deformation and earthquake induced ground hazards: The case of the August 14th 2003 Lefkada earthquake: First International Workshop on Earthquake prediction, Programme with Abstracts, ESC: Greece, Geodynamic Observatory of Athens.

Kokkalas, S., Xypolias, P., and Koukouvelas, I., 2008, Surface ruptures of the recent Mw 6.3 (8 June 2008) earthquake event in the northwestern Peloponnese: A preliminary field report: http://www.emsc-csem.org/index.php?page=current&sub=recent&evt=20080608 _GREECE.

Kokkalas, S., Xypolias, P., Koukouvelas, I.K., and Doutsos, T., 2006, Post-Collisional Contractional and Extensional Deformation in the Aegean Region, *in* Dilek, Y., and Pavlides, S., eds., Post-Collisional Tectonics and Magmatism in the Mediterranean region and Asia: Geological Society of America Special Paper 409, p. 97–123.

Koukouvelas, I.K., 1998, The Egion fault, earthquake-related and long-term deformation, Gulf of Corinth, Greece: Journal of Geodynamics, v. 26, p. 501–513.

Koukouvelas, I., Mpresiakas, A., Sokos, E., and Doutsos, T., 1996, The tectonic setting and earthquake hazards of the 1993 Pyrgos earthquake, Peloponnese, Greece: Journal of the Geological Society London, v. 153, p. 39–49.

Lagios, E., Sakkas, V., Papadimitriou, P., Parcharidis, I., Damiata, B.N., Chousianitis, K., and Vassilopoulou, S., 2007, Crustal deformation in the Central Ionian Islands (Greece): Results from DGPS and DInSAR analyses (1995–2006): Tectonophysics, v. 444, p. 119–145.

Lee, Y-H., Hsieh, M-L., Lu, S-D., Shih, T-S., Wu, W-Y., Sugiyama, Y., Azuma, T., and Kariya, Y., 2002, Slip vectors of the surface rupture of the 1999 Chi-Chi earthquake, western Taiwan: Journal of Structural Geology, v. 25, p. 1917–1931.

Lekkas, E., Logos, E., Danamos, G., Fountoulis, I., and Adamopoulou, E., 1990, Macroseismic observations after the earthquake of October 16th, 1988 in Kyllini peninsula (N.W. Peloponnesus, Greece): Bulletin of the Geological Society of Greece, v. 25, p. 313–328.

Mantovani, E., Albarello, D., Babbucci, D., and Tamburelli, C., 1992, Recentgeodynamic evolution of the central Mediterranean area (Tortonian to Present): Siena, Tipografia Senese, 88 p.

Megna, A., Barba, S., Santini, S., and Dragoni, M., 2008, Effects of geological complexities on coseismic displacement: hints from 2D numerical modelling: Terra Nova, v. 20, p. 173–179.

Monopolis, D., and Bruneton, A., 1982, Ionian sea (western Greece): Its structural outline deduced from drilling and geophysical data: Tectonophysics, v. 83, p. 227–242.

Papadopoulos, G.A., and Plessa, A., 2000, Magnitude-distance relations for earthquake-induced landslides in Greece: Engineering Geology, v. 58, p. 377–386.

Papadopoulos, G.A., and Profis, T., 1990, Macroseismic observations related with the strong shock of October in NW Peloponnesus, Greece: The important role of the microzonation conditions: Journal of Geodynamics, v. 12, p. 217–231.

Pavlides, S., and Caputo, R., 2004, Magnitude versus faults' surface parameters: Quantitative relationships from the Aegean Region: Tectonophysics, v. 380, p. 159–188.

Rebai, S., Philip, H., and Taboada, A., 1992, Modern tectonic stress field in the Mediterranean region: Evidence for variation in stress directions at different scales: Geophysical Journal International, v. 110, p. 106–140.

Roumelioti, Z., Benetatos, Ch., Kiratzi, A., Stavrakakis, G., and Melis, N., 2004, A study of the 2 December 2002 (M5.5) Vartholomio (western Peloponnese, Greece) earthquake and of its largest aftershocks: Tectonophysics, v. 387, p. 65–79.

Sachpazi, M., Hirn, A., Clément, C., Haslinger, F., Laigle, M., Kissling, E., Charvis, P., Hello, Y., Lépine, J.-C., Sapin, M., and Ansorge, J., 2000, Western Hellenic subduction and Cephalonia Transform: Local earthquakes and plate transport and strain: Tectonophysics, v. 319, p. 301–319.

Sassi, W., and Faure, J.-L., 1996, Role of faults and layer interfaces on the spatial variation of stress regimes in basins: Inferences from numerical modeling: Tectonophysics, v. 266, p. 101–119.

Sieh, K., 1996, The repetition of lage-earthquake ruptures: Proceedings of the National Academy of Sciences of the United States of America, v. 93, p. 3764–3771.

Skourlis, K., and Doutsos, T., 2003, The Pindos Fold and Thrust Belt (Greece): Inversion kinematics of a passive continental margin: International Journal of Earth Sciences, v. 92, p. 891–903.

Sotiropoulos, S., Kamberis, E., Triantaphyllou, M., and Doutsos, T., 2003, Thrust sequences at the central part of the External Hellenides: Geological Magazine, v. 140, p. 661–668.

Stamatopoulos, L., Belluomini, G., Branca, M., Manfra, L., and Voltaggio, M., 1998, 230Th/234U and epimerization dating of Quaternary marine deposits in western Peloponneesus (Greece): Zeitschrift fur Geomorphologie, v. 42, p. 245–253.

Tikoff, B., and Wojtal, S.F., 1999, Displacement control of geologic structures: Journal of Structural Geology, v. 21, p. 959–967.

Tselentis, G.-.A., 1998, Fault Lengths During the Patras 1993 Earthquake Sequence as estimated from the Pulse Width of Initial *P* Wave: Pure and Applied Geophysics, v. 152, p. 75–89.

Underhill, J.R., 1989, Late Cenozoic deformation of the Hellenide foreland, western Greece: Geological Society of America Bulletin, v. 101, p. 613–634.

Wen, X.-Z., Mac, S.-L., Xuc, X.-W., and Hec, Y.-N., 2008, Historical pattern and behaviour of earthquake ruptures along the eastern boundary of the Sichuan-Yunnan faulted-block, southwestern China: Physics of the Earth and Planetary Interiors, v. 168, p. 16–36.

Xypolias, P., and Doutsos, T., 2000, Kinematics of rock flow in a crustal scale shear zone: implication for the orogenic evolution of the SW Hellenides: Geological Magazine, v. 137, p. 81–96.

Xypolias, P., and Koukouvelas, I.K., 2005, Paleostress magnitude in a Fold-Thrust Belt (External Hellenides, Greece): Evidence from twinning in calcareous rocks: Episodes, v. 28, p. 245–251.

Yeats, R.S., Sieh, K., and Allen, C.R., 1997, The Geology of Earthquakes: Oxford, Oxford University Press, 568 p.

Zelilidis, A., Koukouvelas, I., and Doutsos, T., 1988, Neogene paleostress changes behind the forearc fold belt in the Patraikos Gulf area, Western Greece: Neues Jahrbuch fur Geologie und Palaontologie Monatshefte, v. 1988, p. 311–325.

Zygouri, V., Verroios, S., Kokkalas, S., Xypolias, P., and Koukouvelas, I.K., 2008, Scaling properties within the Gulf of Corinth, Greece; comparison between offshore and onshore active faults: Tectonophysics, v. 453, p. 193–210.